HK J Paediatr (new series) 2008;**13**:260-266

Imaging Features of Common Non-nodal Neck Masses in Children

KT ***Wong,*** YYP ***Lee,*** AD ***King,*** AT ***Ahuja***

Abstract Children frequently present with a neck mass and imaging plays an important role in their diagnosis and subsequent management. High-resolution ultrasound is the ideal initial imaging modality of choice as diagnosis can be made in most cases, and cross-sectional imaging such as magnetic resonance imaging and computed tomography serve a supplementary role. This review aims to familiarise paediatricians and radiologists with imaging features of common non-nodal neck masses in children.

Key words Child; Computed tomography; Magnetic resonance imaging; Neck; Ultrasound

Introduction

The assessment of a neck mass in a child requires a careful history and meticulous physical examination. Imaging plays an important role in reaching a pre-operative diagnosis and delineating anatomical location and extent of involvement for planning definitive treatment. High-resolution ultrasound (USG) is non-invasive, inexpensive, readily available in most institutions, and does not involve ionising radiation or require sedation. It is therefore the first investigation of choice in children. Cross-sectional imaging including magnetic resonance imaging (MRI) and computed tomography (CT) serve an important supplementary role. MRI is more superior than USG or CT for detection of acute and chronic blood product within lesions containing haemorrhagic component.

Department of Diagnostic Radiology & Organ Imaging, The Chinese University of Hong Kong, Prince of Wales Hospital, Shatin, N.T., Hong Kong, China

KT **Wong** (黃嘉德) *FRCR*
YYP **Lee** (李艷萍) *FRCR*
AD **King** (金雅桃) *FRCR*
AT **Ahuja** (區皓智) *FRCR*

Correspondence to: Dr AT Ahuja

Received June 5, 2008

This review describes imaging features of paediatric non-nodal neck masses commonly seen in routine clinical practice.

Lumps and Bumps

Thyroglossal Duct Cyst (TDC)

Thyroglossal duct cyst is the most common developmental cyst in the neck, accounting for 70% of all congenital neck lesions.[1] The cysts may occur anywhere along the course of the thyroglossal duct remnant from the base of the tongue to the level of thyroid isthmus, but most commonly are closely related to the hyoid bone. Its typical location in the midline, closely related to the hyoid bone, and upward movement upon anterior tongue protrusion are characteristic clinical findings that aid in their correct clinical diagnosis.

The majority of TDCs are infra-hyoid (25-65%) in location, 15-50% occur at the level of hyoid bone and 20-25% are supra-hyoid in location.[2] Children usually present with a painless midline mass and there is often a history of previous incision and drainage at the site.[3] About 50% present before the age of 10 years.

On ultrasound, TDC may appear as (a) simple cyst with homogeneously anechoic with posterior acoustic enhancement (Figure 1); (b) hypoechoic with internal

debris; (c) heterogeneous, probably due to repeated infections or haemorrhage; or (d) uniformly echogenic pseudosolid appearance due to proteinaceous cystic content secreted by its epithelial lining.[1,4]

On MRI TDC is invariably T2-hyperintense. The signal intensity on T1-weighted sequence is variable due to difference in constituents of the cystic content, with T1-hyperintensity seen in lesions with high proteinaceous content.[5]

Second Branchial Cleft Cyst (BCC)

Second branchial cleft cyst constitutes 95% of all congenital branchial cleft cysts. Its typical location between submandibular gland anteriorly, medial end of the sternocleidomastoid muscle posteriorly, and superficial to the carotid bifurcation allows accurate pre-operative diagnosis.

The ultrasound appearances depend on whether there has been previous infection or haemorrhage. Most uninfected second BCCs demonstrate typical appearances of a cyst in that they are well-defined thin walled and anechoic with no internal debris and show posterior acoustic enhancement. Some cysts may exhibit a pseudosolid appearance with uniform internal echoes due to proteinaceous content such as mucus, debris, lymphocytes, epithelial cells and cholesterol crystals within the cyst.[6] Second BCCs complicated by previous infection/inflammation are usually ill-defined, heterogeneous and thick walled, containing internal debris and septae. These may mimic cystic metastatic nodes and a fine needle aspiration cytology (FNAC) may be indicated to confirm the nature of the lesion.[7]

CT or MRI may be indicated if a sinus or fistula is suspected. On CT, second BCC appears as a well-defined homogenous low attenuation mass in the typical location i.e. posterior to submandibular gland, anterior to major vessels and medial to anterior margin of sternocleidomastoid muscle. An infected cyst can be hyperattenuated with an ill-defined irregular rim, mimicking a metastatic node. On MRI, the T2-weighted signal intensity is invariably high due to presence of intracystic fluid (Figure 2). The presence of

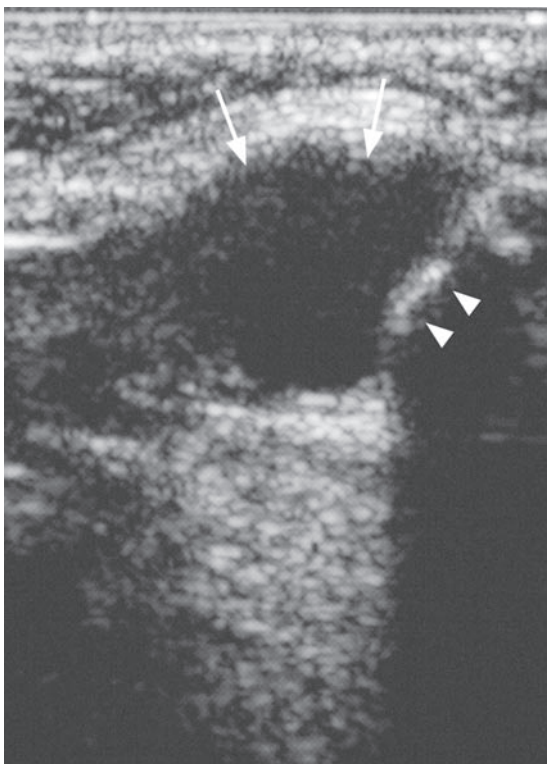

Figure 1 A 3-year-old boy with a thyroglossal duct cyst. Longitudinal gray-scale ultrasound shows a well-defined anechoic cyst (arrows) in the midline of the neck located just above the hyoid bone (arrowheads).

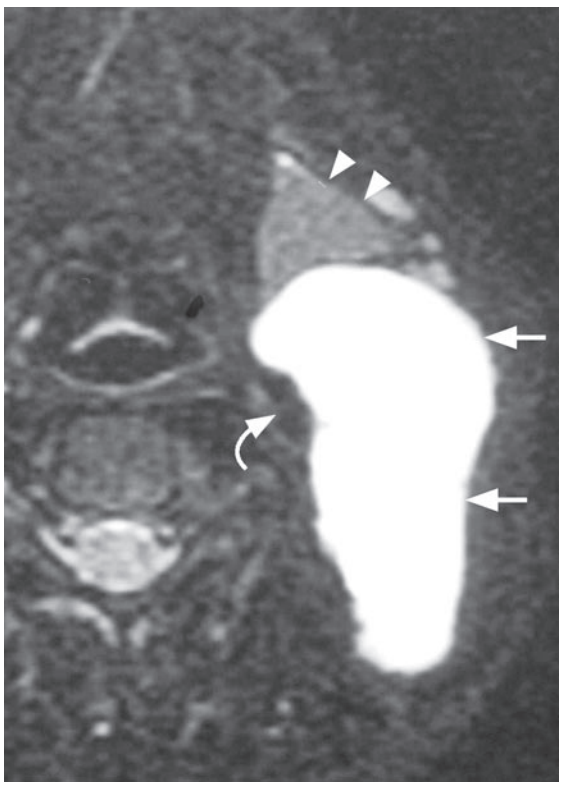

Figure 2 An 11-year-old girl with a second branchial cleft cyst. Fat-suppressed T2-weighted axial MR shows a well-circumscribed cyst (arrows) which is homogeneously hyperintense. Note its typical location posterior to the left submandibular gland (arrowheads) and superficial to the carotid sheath (curved arrow).

proteinaceous content of the cyst may sometimes cause it to appear hyperintense rather than isointense or hypointense on T1-weighted sequence.[8]

Cystic Hygroma

Cystic hygroma is the most commonly encountered type of lymphangioma. 50-60% present at birth or perinatally, another 30% present by 2 years of age.[9] They usually present clinically as a painless compressible neck mass, more commonly in the posterior triangle. Following haemorrhage, they can enlarge rapidly and become tense. The primary role of imaging is to confirm the clinical diagnosis and delineate anatomical extent prior to surgery or sclerotherapy (as large lesions are commonly transpatial i.e. involve more than one anatomical space).

On ultrasound, cystic hygroma appears as a compressible multiloculated cystic lesion with intervening thin septae (Figure 3). Vascularity may be seen within the septa. Large lesions tend to be transpatial and follow no obvious anatomical boundaries. If there has been a previous episode of haemorrhage or infection, the cyst walls are irregular and the lesion contains low level internal echoes or hyperechoic debris.[8,10,11]

While the diagnosis can easily be obtained by ultrasound, MRI is often required to accurately map the anatomical extent of involvement. T2-weighted scans offer superb contrast resolution for delineation of extent of cystic hygroma, which invariably appears as high signal intensity mass with multiple internal septae (Figure 4).[8,12] In patients treated by sclerotherapy with OK-432 (Picibanil) injection, serial MRI helps to assess treatment response and the necessity for repeated injections.[13,14]

Dermoid / Epidermoid Cyst

Approximately 7% of dermoid cysts occur in the head and neck. They are frequently midline in location, typically in the floor of mouth deep to the mylohyoid muscle, and in the suprasternal notch. It may also occur in the orbit, nasal and oral cavities.

On ultrasound, an epidermoid cyst is usually well-defined anechoic with posterior acoustic enhancement, midline in location.[8,9,11] Due to the presence of cellular material within the cyst, it may exhibit a pseudosolid appearance on ultrasound with uniform homogeneous

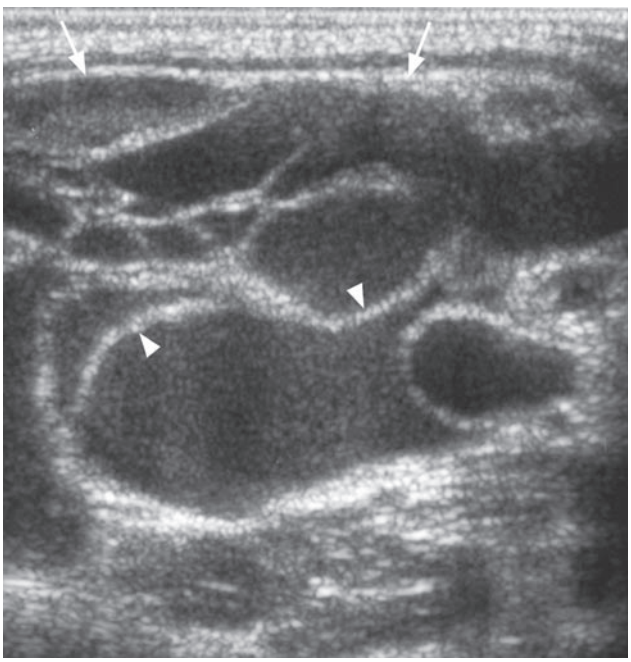

Figure 3 An 1-year-old boy with cystic hygroma. Transverse gray-scale ultrasound shows a large cystic lesion (arrows) with multiple septations (arrowheads) in the posterior triangle. MRI is indicated to evaluate the extent of such lesion as they are frequently trans-spatial in distribution.

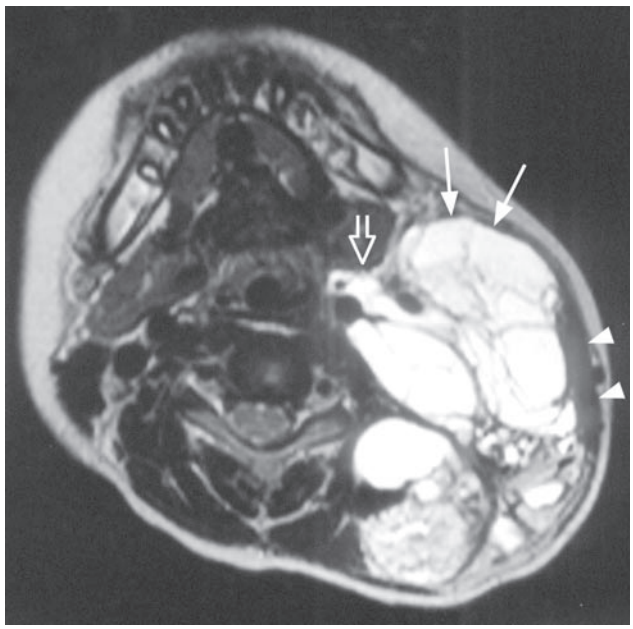

Figure 4 An 8-year-old girl with cystic hygroma. Axial T2-weighted MR shows a large multi-septated cystic lesion (arrows) in the left posterior triangle underneath the left sternocleidomastoid muscle which is elevated (arrowheads). Note the transpatial nature of cystic hygroma with extension to adjacent left carotid space (open arrow). The exact anatomical distribution is better defined with MR than ultrasound for large transpatial lesion.

internal echoes (Figure 5). Dermoid cysts may have mixed internal echoes due to its fat content and the presence of osseo-dental structures within, seen as echogenic foci with dense posterior acoustic shadowing.

On CT or MRI, globules of fat floating within the lesion may produce a characteristic "sack of marbles" appearance. Fat and/or fluid levels may be present. Both CT and MRI offer clear delineation of the anatomical location and extent of involvement.[8,9]

Venous Vascular Malformation (VVM)

Approximately 15% of VVMs occur in the head and neck region, masseter muscle is the commonest site of involvement. Ultrasound appearances are fairly characteristic: mass with a hypoechoic, heterogeneous echopattern with multiple sinusoidal spaces (Figure 6). Phleboliths (dense echogenic foci casting posterior acoustic shadowing) are seen in 22% of cases.[15,16] While Power Doppler may depict the slow flowing nature of venous vascular malformation, the flow phenomenon is usually better demonstrated on real time gray-scale ultrasound.

On MRI, venous vascular malformation shows a characteristic high signal on T2-weighted fat saturated sequence ensuring its conspicuity (Figure 7).[15] Although MRI may not be as sensitive as ultrasound in the identification of phleboliths, it is excellent (better than CT and ultrasound) at depicting the full extent of large venous vascular malformation which may be trans-spatial.

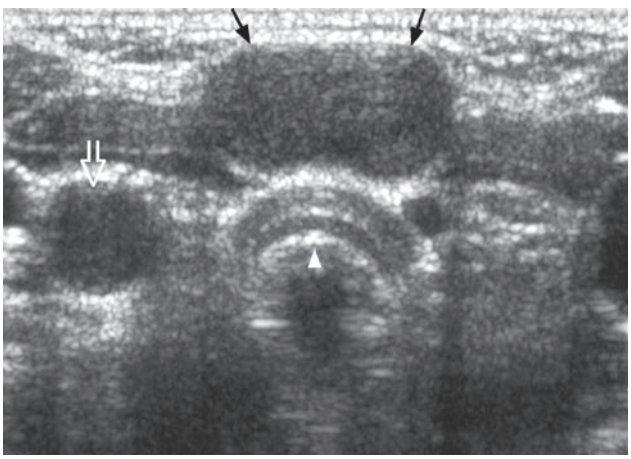

Figure 5 A 7-year-old girl with epidermoid cyst. Transverse gray-scale ultrasound shows a well-defined midline cystic lesion with 'pseudo-solid' appearances in suprasternal notch (arrows). Arrowhead – trachea, open arrow – right common carotid artery.

Abscess

In the antibiotics era, the incidence of neck abscess is low. It is usually due to underlying causes such as acute lymphadenitis and sialadenitis. On USG an abscess appears as ill-defined, irregular fluid collection with thick walls and internal debris (Figure 8).[11] The adjacent soft tissue and subcutaneous layer may appear edematous.

On CT, an abscess usually appears as a uniloculated/ multi-loculated low attenuation lesion with rim enhancement. Internal gas collections may be present, and the adjacent subcutaneous and fascial fat planes are commonly obliterated.[17] On MRI, an abscess typically has low T1-weighted and high T2-weighted signal intensities. Rim or thick peripheral enhancement is often seen in a mature neck abscess.[17]

Ultrasound helps to confirm the clinical diagnosis of abscess, delineate its anatomical location prior to surgery or aspiration, identify complications such as venous thrombosis or carotid involvement and provide real-time imaging guidance for aspiration.

Lesions of Thyroid Gland

Acute Suppurative Thyroiditis (AST)

The thyroid gland is remarkably resistant to infection because of its thick fibrous capsule and high iodine content. AST most commonly affects children with associated

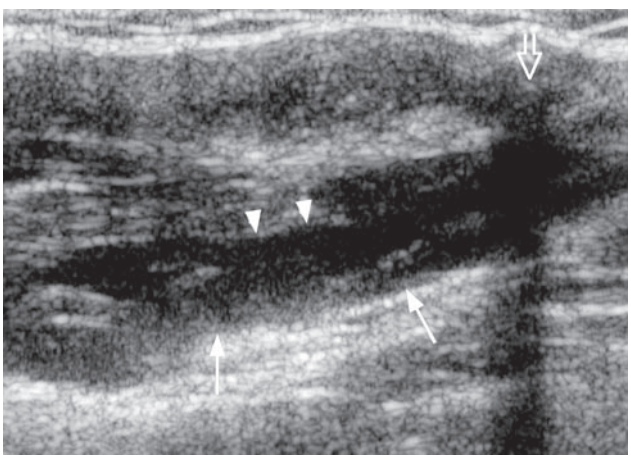

Figure 6 An 8-year-old boy with venous vascular malformation in right submandibular region. Transverse gray-scale ultrasound shows a well-defined hypoechoic lesion (arrows) with multiple sinusoidal spaces (arrowheads) and phlebolith (open arrow) casting marked posterior acoustic shadowing. Slow flow is also demonstrated on real-time gray scale examination.

Figure 7 An 8-year-old boy with venous vascular malformation in right submandibular region. Fat-suppressed T2-weighted coronal MR shows a lobulated homogeneous hyperintense lesion (arrows) with foci of signal void (arrowhead) due to the presence of phlebolith.

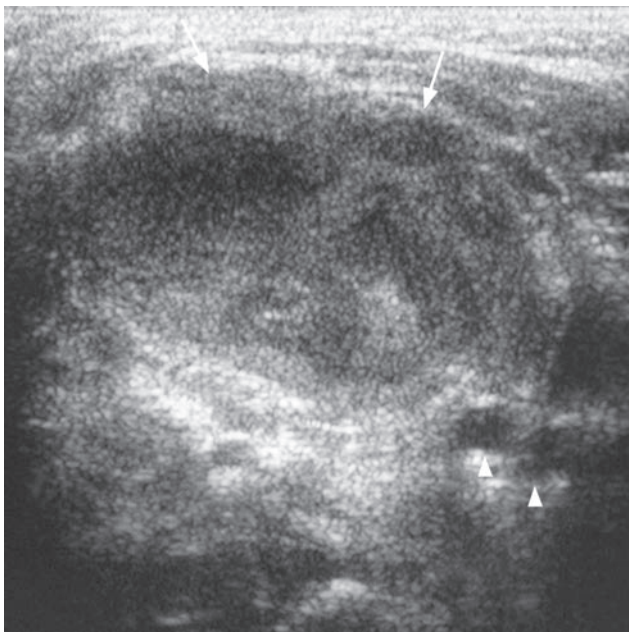

Figure 8 A 5-month-old girl with neck abscess. Transverse gray-scale ultrasound shows an ill-defined, irregular, heterogeneous, hypoechoic fluid collection with internal debris (arrows) in right upper neck adjacent to the carotid bifurcation (arrowheads).

piriform fossa sinus, and the infection usually begins in perithyroidal soft tissues and secondarily involves the thyroid gland.

On ultrasound, both intra- and extra-thyroid abscesses are seen as ill-defined, hypoechoic, heterogeneous lesions with internal debris and thick walls. Occasionally tiny echogenic foci with reverberation artifacts due to presence of gas bubbles may be seen. The fascial planes between the thyroid gland and perithyroidal soft tissue are obliterated.[11,18] Adjacent inflammatory lymph nodes are frequently present. Apart from diagnosis, ultrasound serves as real-time guide for needle aspiration if necessary and to monitor response to antibiotics treatment.

In complicated cases or if there is suboptimal response to medical treatment, CT helps in the exact anatomical delineation of the suppurative process prior to surgical drainage (Figure 9). A barium swallow study is required to identify the associated piriform fossa sinus.[18] CT and MRI have also been used to demonstrate the presence of abscess and fistula tract from the piriform fossa.[19,20]

Papillary Carcinoma

Thyroid carcinoma is an uncommon malignancy in children, but is unique in having an overall favourable prognosis despite its relative high rate of nodal and distant metastases. Papillary carcinoma is the commonest histological subtype. Most children present with a palpable neck mass. On USG it appears as solitary hypoechoic nodule with ill-defined margins. The presence of punctate calcifications within the nodule further supports the diagnosis of papillary carcinoma.[21,22] USG also helps to detect regional lymphadenopathy prior to surgery, provide real time guidance for FNAC and is a useful tool in the post-operative follow-up of these children.

Lesions of Major Salivary Glands

Acute Sialadenitis/Abscess

Children usually present with a painful swelling in the parotid/submandibular regions. On USG, the inflamed salivary gland shows diffuse glandular enlargement with heterogeneous hypoechoic parenchymal echopattern (Figure 10).[23,24] Progression to an abscess results in an ill-defined thick-walled hypoechoic lesion with internal debris. USG-guided fine needle aspiration helps to confirm diagnosis and bacteriological culture to guide appropriate antibiotics treatment.

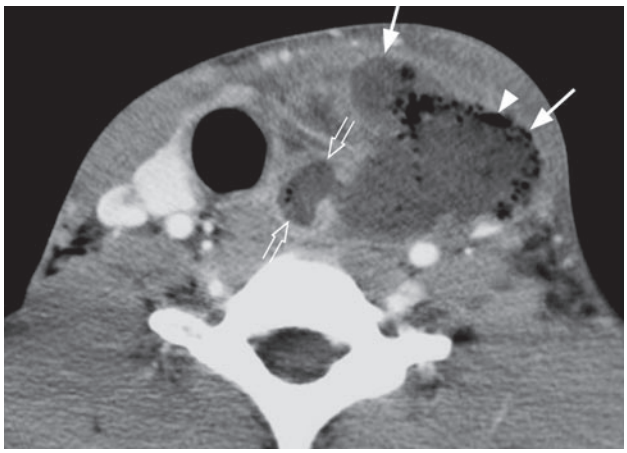

Figure 9 A 2-year-old boy with acute suppurative thyroiditis. Contrast-enhanced CT shows a fluid collection (arrows) with internal gas (arrowhead) involving left lobe of thyroid gland (open arrows) and adjacent soft tissue.

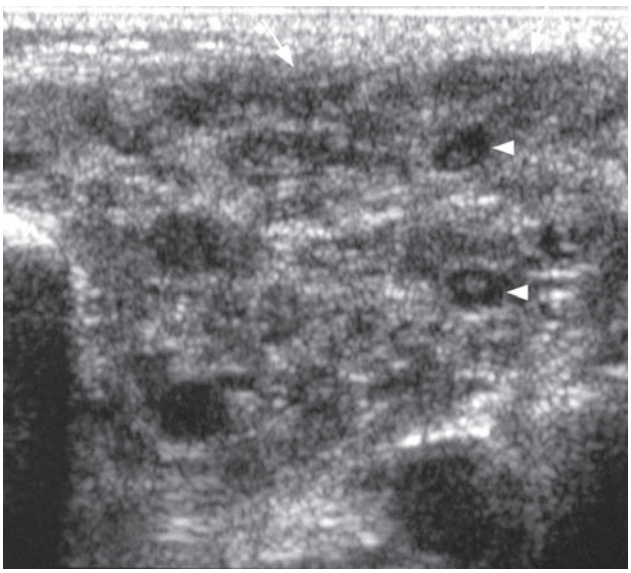

Figure 10 A 5-year-old boy with acute parotid sialadenitis. Transverse gray-scale ultrasound shows diffuse enlargement of left parotid gland with heterogeneous nodular hypoechoic echopattern (arrow). Note the small, prominent, intra-parotid nodes (arrowheads).

Infantile Haemangioma

Infantile haemangioma is the most common parotid gland tumour of childhood. On USG it appears as a homogeneous mass enlarging and replacing most or all of the visualised parotid gland, with a lobular internal structure, fine echogenic internal septations, and a mildly lobulated contour. Color Doppler and power Doppler imaging shows extremely high vascularity within the mass. Large well-defined lesion with uniform intense contrast enhancement is the most common MRI finding (Figure 11).[25]

Figure 11 A 2-month-old boy with infantile haemangioma of right parotid gland. Fat-suppressed T2-weighted axial MR shows a well-defined hypervascular lesion with marked homogeneous enhancement (arrow) occupying the right parotid gland.

Conclusion

In a child presenting with a neck lump, high resolution ultrasound is an ideal initial imaging investigation to characterise the lesion. In addition, it provides real-time guidance for safe FNAC/biopsy to enhance the diagnostic accuracy. For large deep-seated and/or large lesions assessment with MRI/CT is essential to delineate the exact anatomical extent of the lesion.

References

1. Ahuja AT, King AD, Metreweli C. Sonographic evaluation of thyroglossal duct cysts in children. Clin Radiol 2000;55:770-4.
2. Telander RL, Filston HC. Review of head and neck lesions in infancy and childhood. Surg Clin North Am 1992;72:1429-47.

3. Filston HC. Common lumps and bumps of the head and neck in infants and children. Pediatr Ann 1989;18:180-6.
4. Ahuja AT, Wong KT, King AD, Yuen EH. Imaging for thyroglossal duct cyst: the bare essentials. Clin Radiol 2005;60:141-8.
5. Ahuja AT, King AD, King W, Metreweli C. Thyroglossal duct cysts: sonographic appearances in adults. AJNR Am J Neuroradiol 1999;20:579-82.
6. Ahuja AT, King AD, Metreweli C. Second branchial cleft cysts: variability of sonographic appearances in adult cases. AJNR Am J Neuroradiol 2000;21:315-9.
7. Ahuja A, Ng CF, King W, Metreweli C. Solitary cystic nodal metastasis from occult papillary carcinoma of the thyroid mimicking a branchial cyst: a potential pitfall. Clin Radiol 1998; 53:61-3.
8. Koeller KK, Alamo L, Adair CF, Smirniotopoulos JG. Congenital cystic masses of the neck: radiologic-pathologic correlation. Radiographics 1999;19:121-46.
9. Som PM, Smoker WR, Curtin HD, et al. Congenital lesions. In: Som PM, Curtin HD, eds. Head and Neck Imaging, 4th edition. St Louis: Mosby Year Book, 2003;1828-64.
10. Lev S, Lev MH. Imaging of cystic lesions. Radiol Clin North Am 2000;38:1013-27.
11. Ahuja AT. Lumps and bumps in the head and neck. In: Ahuja AT, Evans RM, eds. Practical Head and Neck Ultrasound. London: Greenwich Medical Media Limited, 2000;87-104.
12. Siegel MJ, Glazer HS, St Amour TE, Rosenthal DD. Lymphangiomas in children: MR imaging. Radiology 1989;170: 467-70.
13. Giguère CM, Bauman NM, Sato Y, et al. Treatment of lymphangiomas with OK-432 (Picibanil) sclerotherapy: a prospective multi-institutional trial. Arch Otolaryngol Head Neck Surg 2002;128:1137-44.
14. Bloom DC, Perkins JA, Manning SC. Management of lymphatic malformations. Curr Opin Otolaryngol Head Neck Surg 2004; 12:500-4.
15. Ahuja AT, Richards P, Wong KT, Yuen EH, King AD. Accuracy of high-resolution sonography compared with magnetic resonance imaging in the diagnosis of head and neck venous vascular malformations. Clin Radiol 2003;58:869-75.
16. Yang WT, Ahuja A, Metreweli C. Sonographic features of head and neck hemangiomas and vascular malformations: review of 23 patients. J Ultrasound Med 1997;16:39-44.
17. Smoker WR. Oral Cavity. In: Som PM, Curtin HD, eds. Head and Neck Imaging, 4th edition. St Louis: Mosby Year Book, 2003; 1377-464.
18. Ahuja AT, Griffiths JF, Roebuck DJ, et al. The role of ultrasound and oesophagography in the management of acute suppurative thyroiditis in children associated with congenital pyriform fossa sinus. Clin Radiol 1998;53:209-11.
19. Sai Prasad TR, Chong CL, Mani A, et al. Acute suppurative thyroiditis in children secondary to pyriform sinus fistula. Pediatr Surg Int 2007;23:779-83.
20. Wang HK, Tiu CM, Chou YH, Chang CY. Imaging studies of pyriform sinus fistula. Pediatr Radiol 2003;33:328-33.
21. Simeone JF, Daniels GH, Mueller PR, et al. High-resolution real-time sonography of the thyroid. Radiology 1982;145:431-5.
22. Ahuja AT. The thyroid and parathyroids. In: Ahuja AT, Evans RM, eds. Practical Head and Neck Ultrasound. London: Greenwich Medical Media Limited, 2000;35-64.
23. Bradley MJ. Salivary glands. In: Ahuja AT, Evans RM, eds. Practical Head and Neck Ultrasound. London: Greenwich Medical Media Limited, 2000;17-33.
24. Garcia CJ, Flores PA, Arce JD, Chuaqui B, Schwartz DS. Ultrasonography in the study of salivary gland lesions in children. Pediatr Radiol 1998;28:418-25.
25. Roebuck DJ, Ahuja AT. Hemangioendothelioma of the parotid gland in infants: sonography and correlative MR imaging. AJNR Am J Neuroradiol 2000;21:219-23.